



# Microdosimetry in BNCT

Valeria Conte<sup>1</sup> · Anna Bianchi<sup>1</sup> · Anna Selva<sup>1</sup>

Received: 16 January 2024 / Accepted: 16 February 2024 / Published online: 28 February 2024

© The Author(s) under exclusive licence to International Union for Physical and Engineering Sciences in Medicine (IUPESM) 2024

## Abstract

**Purpose** This paper explores the application of microdosimetry in the context of Boron Neutron Capture Therapy (BNCT). In particular it aims to elucidate the crucial role of microdosimetry in measuring dose enhancement resulting from elevated boron-10 concentrations in tumor cells during BNCT.

**Methods** A critical survey on microdosimetry is first given, to underline the relevance of the stochastic fluctuations of the radiation interactions at the microscopic level. Successively, the methodology of microdosimetric application to BNCT is reviewed. Significant examples are reported that help understanding the potentialities of microdosimetry on BNCT. The analysis involves examining the energy spectra in mixed radiation fields, taking into account both small and large energy events influenced by the stopping power and range of the particle.

**Results** The findings of this study reveal valuable insights into the contribution of microdosimetry in BNCT. The analysis of energy spectra enables the differentiation of various components within the radiation field, both in terms of dose and of biological effectiveness. The results shed light on the dose enhancement attributed to higher concentrations of boron-10 in tumor cells, providing a comprehensive understanding of the biological effectiveness of boron neutron capture reaction products.

**Conclusions** This paper underscores the pivotal role of microdosimetry in BNCT, emphasizing its capability to unravel the intricacies of energy deposition and dose distribution at the micrometric scale. The application of microdosimetry emerges as a valuable tool in optimizing BNCT protocols and advancing our comprehension of radiation effects in targeted cancer therapy.

**Keywords** Microdosimetry · Boron neutron capture therapy · Tissue equivalent proportional counters · Dosimetry

## 1 Introduction

Microdosimetry focuses on studying how energy is randomly deposited in tiny, sub-nuclear cellular structures like chromosomes. It is important to note that microdosimetry is not merely small-scale dosimetric-investigation; it is about

characterizing the random fluctuations of energy deposited event by event.

Figure 1 illustrates the difference in energy deposition patterns between low and high Linear Energy Transfer (LET) radiation. The larger circles in the figure symbolize microscopic target volumes, while red dots represent fixed-sized energy depositions. On the left, each target has a single dot, demonstrating a homogeneous distribution. The background is uniform light-yellow, emphasizing the uniformity in energy distribution. On the right, some areas have multiple red dots (representing high energy deposition), while others have only a few or none, indicating a heterogeneous distribution. Areas with higher energy deposition are shaded in red, indicating clustered DNA damage due to high Linear Energy Transfer (LET) radiation. Despite both sides having an average of, let's say, 1 Gy of absorbed dose, the distribution pattern plays a significant role. Small energy deposits generally result in simple DNA damages that are easily repairable. Conversely, larger energy depositions over shorter distances can cause clustered DNA damage that cells struggle to repair effectively

---

Anna Bianchi and Anna Selva contributed equally to this work.

---

This article is part of the Hadrontherapy and BNCT: Current Status and Future Trends

---

✉ Valeria Conte  
valeria.conte@lnl.infn.it

Anna Bianchi  
anna.bianchi@lnl.infn.it

Anna Selva  
anna.selva@lnl.infn.it

<sup>1</sup> Istituto Nazionale di Fisica Nucleare, Laboratori Nazionali di Legnaro, Viale dell'Università 2, Legnaro, (PD), Italy

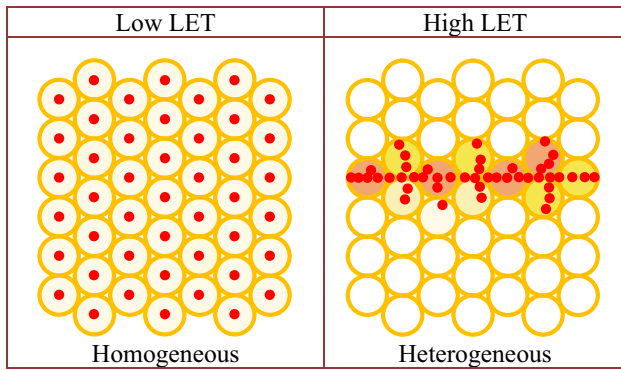


**Fig. 1** Representation of two irradiations at 1 Gy. Left: Low Linear Energy Transfer (LET) radiation shows a uniform microscopic distribution. Right: High LET radiation displays a heterogeneous distribution of energy deposition, where some targets experience substantial energy deposition events while others have few or no energy depositions. The color intensity represents the severity of biologically induced damage

[1]. The severity of this damage is represented in Fig. 1 by the color intensity of the targets.

In microdosimetry, a commonly used quantity is the lineal energy,  $y$ . It is defined as the ratio of the energy imparted by a single event,  $\epsilon_s$ , to the mean chord length of the target volume,  $\bar{l}$ . The formula is:

$$y = \frac{\epsilon_s}{\bar{l}} \tag{1}$$

Lineal energy is expressed in units of  $\text{keV } \mu\text{m}^{-1}$ . Being a stochastic quantity, the lineal energy is characterized by a probability density distribution,  $f(y)$ . The dose probability density of  $y$ ,  $d(y)$ , is even more important and is obtained as

the product of the frequency of a given event size by the size of the event, normalized to unit area:

$$d(y) = \frac{yf(y)}{\int_0^\infty yf(y)dy} \tag{2}$$

More details on microscopic quantities definitions and their relation to macroscopic quantities like the absorbed dose and the LET can be found in the ICRU Reports on Microdosimetry [2, 3]. Notably, the new ICRU Report 98 recommends considering the stochastic nature of radiation interactions, when the mean number of charged particles, including delta rays originating outside the site, interacting with the volume of interest is small. Furthermore, it is explained that in mixed radiation fields, the fluence of the higher LET components should be considered. This specific case applies to BNCT, because the high LET components related to alpha particles and lithium ions emerging from the neutron capture reaction have a small fluence, albeit contributing significantly to the dose. The situation is illustrated in Fig. 2, which is divided into two parts labeled “High fluence” and “Low fluence”. In both parts, small circles represent volumes of interest where radiation interactions occur. Under “High fluence”, there are many arrows indicating many low LET charged particles interacting with each volume. In this case microdosimetry is not necessary because the resulting distribution of the imparted energy is rather homogenous. Under “Low fluence”, fewer arrows indicate that a small number of high LET charged particles interact with each volume, resulting in a heterogeneous distribution of energy imparted. Here, microdosimetry is necessary to study the stochastic nature of these

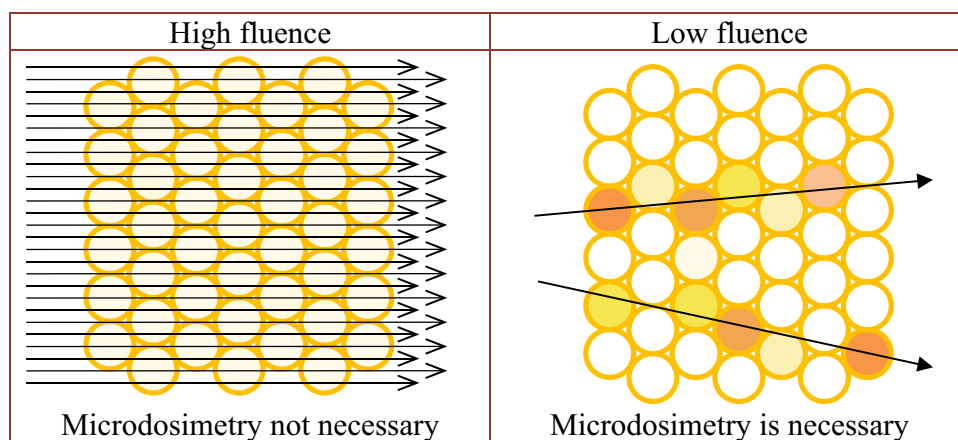


**Fig. 2** Schematic illustration of when a microdosimetric study of the stochastic nature of radiation interactions is recommended. The volume of interest is represented by each small circle. Left: the mean number of charged particles interacting with the volume of interest is large, albeit the corresponding absorbed dose is rather low due to

low LET of particles. Right: the mean number of high LET charged particles interacting with the volume of interest is small and results in a heterogeneous distribution of the energy imparted. In this case the stochastic nature of radiation interactions should be considered

interactions. The color intensity within circles under “Low fluence” varies, visually representing the heterogeneous distribution of energy.

In the literature, the majority of studies focus on computational microdosimetry, utilizing Monte Carlo tools for investigating various irradiation conditions. For example, Nichols et al. [4] developed an enhanced tissue model to elucidate observed differences in clinical outcomes based on tissue cellular geometry and the influence of neighboring cells. More recently, Sato et al. [5] proposed a novel microdosimetric model for biological effectiveness in BNCT, considering intra- and intercellular heterogeneity in  $^{10}\text{B}$  distribution. Hu et al. [6] successfully validated the PHITS Monte Carlo simulation code against experimental data obtained using a TEPC. They concluded that PHITS can accurately calculate thermal neutron fluxes, gamma-ray dose rates, and RBE when physical measurements pose challenges. Moreover, building on the pioneering work by Wu et al. [7], several experimental studies were conducted in reactor-based BNCT fields using both standardized TEPCs [8–12] and miniaturized TEPCs suitable for intense radiation fields [13–15]. Silicon microdosimeters have also demonstrated success [16, 17], and more recently, experimental techniques have been implemented for characterizing accelerator-based neutron sources for BNCT [18–20]. This work provides a comprehensive

survey of the methodology and sheds light on the potential advantages that microdosimetry offers in terms of determining dose components and assessing RBE.

## 2 Methods

Experimental microdosimetry in BNCT relies on the dual-counter technique initially introduced by Wu et al. [7]. This method entails conducting paired measurements with two TEPCs that are identical except for their boron content. One detector lacks boron, while the other has cathode walls doped with boron. The experimental setup is illustrated in Fig. 3, which displays two identical TEPCs, one without boron and the other with boron-doped cathode walls, as depicted in the right-side drawings.

Microdosimetric lineal energy spectra measured in a thermal neutron field without and with boron at  $1\ \mu\text{m}$  simulated site sizes are shown in Fig. 4. More details on the experimental setup and radiation field can be found in [19]. The dose probability distributions were normalized, as per Eq. (2); therefore, in this graphical representation, equal areas under the curve correspond to equal fractions of the total dose [2, 3]. In both spectra the low LET component, mainly due to unavoidable gamma rays, is distinguishable

**Fig. 3** The microdosimetric dual-counter technique uses two TEPCs that are identical, differing only in boron content: one with boron-doped cathode walls and the other without. The two microdosimeters shown on the left side of the figure were constructed at Legnaro National Laboratories (LNL) of Istituto Nazionale di Fisica Nucleare (INFN) and feature a cylindrical sensitive volume measuring 1 mm in diameter and height

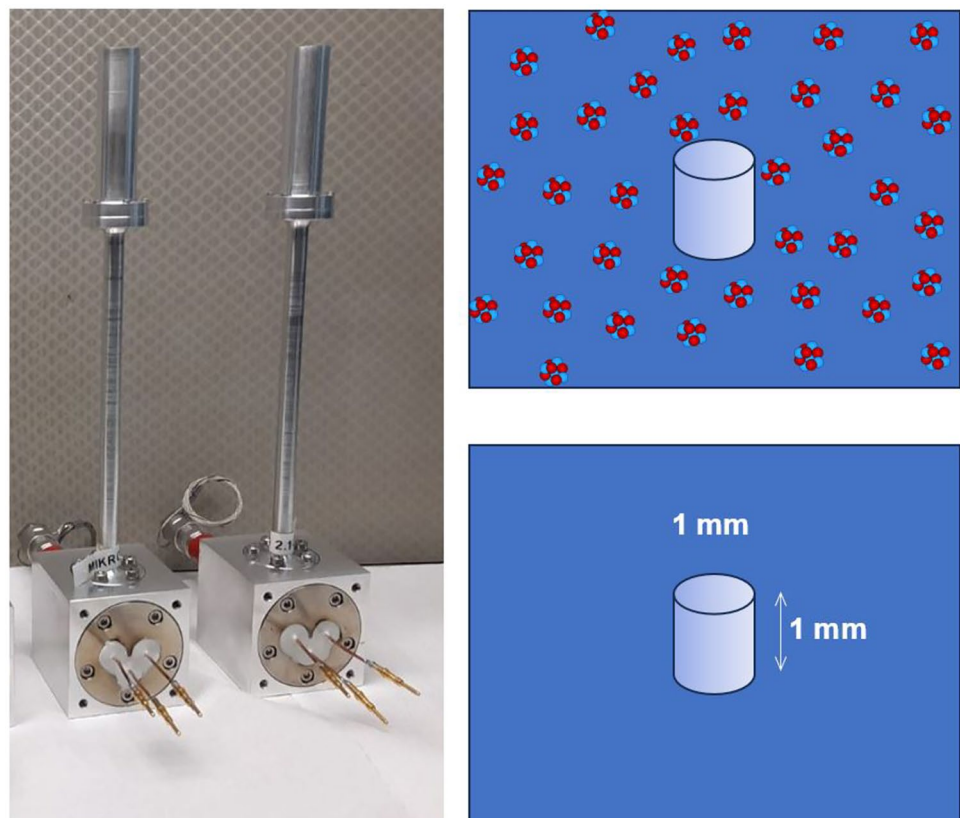
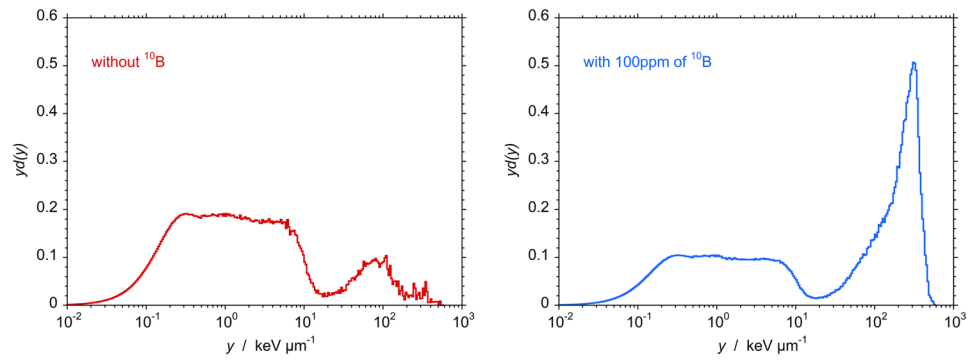


**Fig. 4** Microdosimetric spectra measured in a mixed thermal neutron and gamma radiation field at a simulated site size of 1 mm. The left spectrum was measured with a TEPC without boron, while the right spectrum was measured with a TEPC with cathode walls doped at 100 ppm of  $^{10}\text{B}$ . Data adapted from [19]



below approximately  $15 \text{ keV } \mu\text{m}^{-1}$ , while the events above this threshold are due to neutron interactions.

The lineal energy distributions presented in Fig. 4 are analyzed, considering that the radiation spectra (below approximately  $15 \text{ keV } \mu\text{m}^{-1}$ ) should be nearly identical, irrespective of boron content. Figure 5 illustrates this. The left panel shows different gamma components, with the gamma portion being lower in the spectrum with boron. This is a consequence of the normalization procedure on  $d(y)$ . The areas subtended by the two curves (0 and 100 ppm of  $^{10}\text{B}$ ) are equal and correspond to an absorbed dose of, let's say, 1 Gy. However, the absolute value of the dose contribution due to gamma radiation should be the same in both cases. If we want to calculate the relative dose enhancement due to the boron neutron capture (BNC) reactions, the spectrum with boron must be multiplied by a constant factor to align its gamma region to that without boron, as shown in the right side of Fig. 5. In this case the area subtended by the curve without  $^{10}\text{B}$  is still 1 Gy, while the additional area subtended by the

curve with 100 ppm of  $^{10}\text{B}$  represents the dose enhancement due to the BNC reactions.

By subtracting the spectrum without  $^{10}\text{B}$  from the one with  $^{10}\text{B}$ , the resulting distribution represents the contribution of BNC products, specifically alpha particles and lithium ions. Figure 6 shows this distribution, labelled as the “pure BNC component”.

A recent work by Conte et al. [21] confirmed experimentally that the dose enhancement due to BNC interactions is proportional to the  $^{10}\text{B}$  concentration, while the individual microdosimetric distribution of the lineal energy is invariant with boron content. The proportionality factor has not a unique value but depends on the total distribution, and specifically on the gamma and fast neutron components of the investigated radiation field. For instance, for the distribution shown in Fig. 6, the BNC dose enhancement amounts to approximately 84% of the dose without boron. Referring to the  $^{10}\text{B}$  concentration of 100 ppm, this number leads to a proportionality factor of about  $7.7 \times 10^{-3}$  per ppm of boron. Based on these findings, the impact of BNCT in the tumor treatment

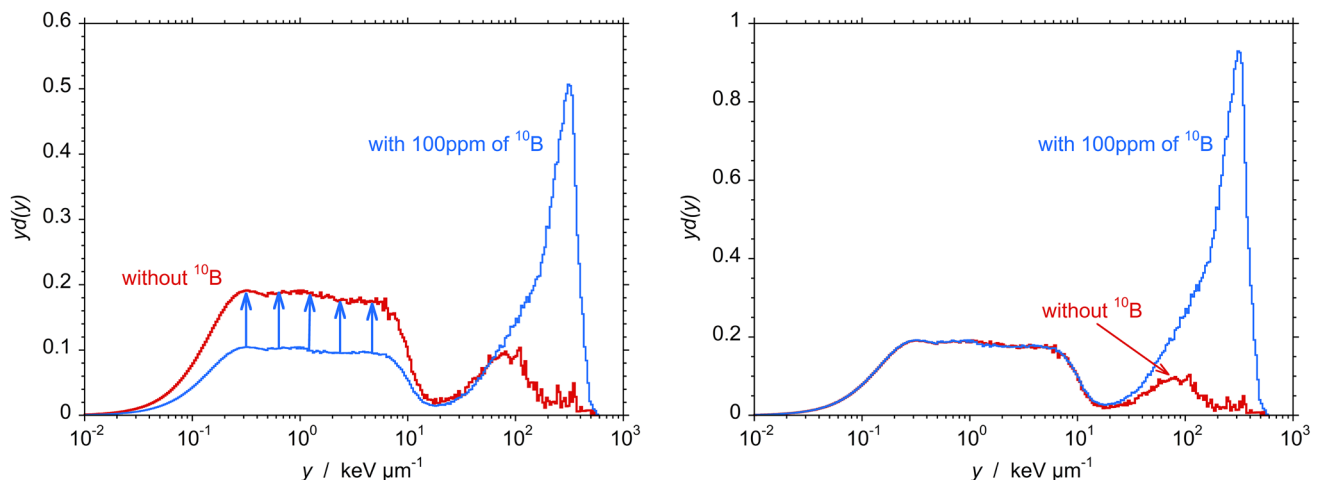


**Fig. 5** Microdosimetric spectra measured with and without boron. In the left panel both distributions  $d(y)$  are normalized to the unit dose. In the right panel the spectrum with boron has been multiplied by a

constant factor to align its gamma component to that without boron. Data adapted from [19]

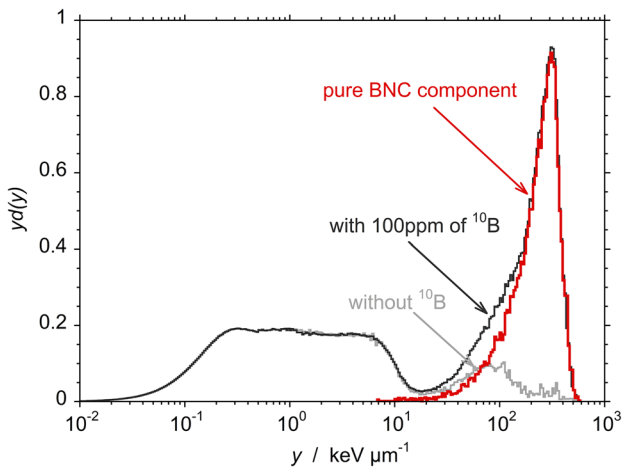
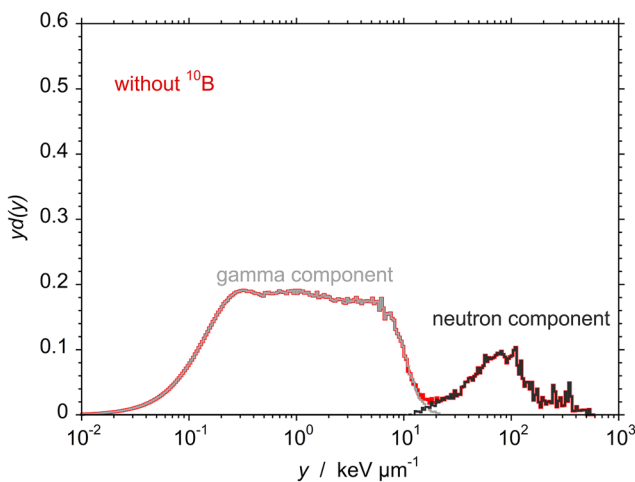


**Fig. 6** The “pure BNC component” is obtained by subtracting the spectrum without boron from the one with boron. Data adapted from [19]

region as well as in the healthy tissue can be easily evaluated. In this work, a desirable [23] tumor:normal tissue ratio of 3.5:1 was considered, specifically with concentrations of 20 and 70 ppm of <sup>10</sup>B in normal and tumor tissues, respectively.

In addition to the pure BNC component, the gamma and total neutron components (both with and without BNC reactions) can also be evaluated. The gamma component is obtained by merging the shoulder of the spectrum corresponding to the e-edge with a pure gamma spectrum, for instance, that produced from a <sup>137</sup>Cs gamma source. The neutron components are obtained by subtracting the gamma portion from the entire spectra. An example of the gamma and neutron components are highlighted in Fig. 7.



Finally, the relative biological effectiveness (RBE) of the radiation field can be estimated based on the measured microdosimetric spectra. The procedure consists of weighting the total and the individual lineal energy distributions  $d(y)$  with a lineal energy dependent weighting function  $r(y)$  to determine the effective RBE, neutron\_RBE, photon\_RBE and BNC\_RBE:

$$RBE = \int_0^{\infty} r(y)d(y)dy \tag{3}$$

Weighting functions  $r(y)$  are determined by combining data from biological experiments and microdosimetric distributions, and in general depend on the biological end point under consideration. In this work we used the weighting function derived from Tilikidis [22] using RBE values at 2 Gy for jejunum crypt cell survival obtained in therapeutic fast neutron beams and in low-energy neutron beams. This function has been already used in other studies focused on BNCT, leading to microdosimetric assessment of the RBE that is in reasonable agreement with biological data [6, 10, 11]. Minor differences have been evidenced when using other weighting functions [20].

### 3 Results and discussion

Following the procedure outlined in the "Methods" section and assuming a tumor-to-normal (T/N) tissue ratio of 3.5:1 for the <sup>10</sup>B concentration, with a concentration of 20 ppm in normal tissue, the concentration in tumor cells was calculated to be 70 ppm. This ratio has been assumed because it is the typical value obtained in clinical trials using

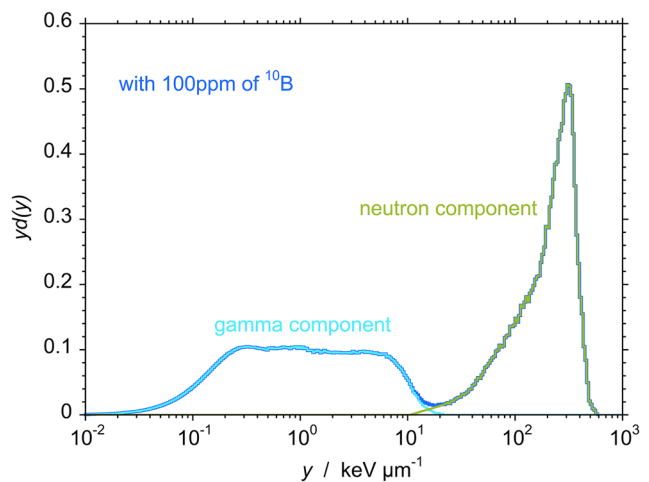


**Fig. 7** The gamma and neutron components of the microdosimetric spectra measured without (left) and with 100 ppm of <sup>10</sup>B (right). Data adapted from [19]

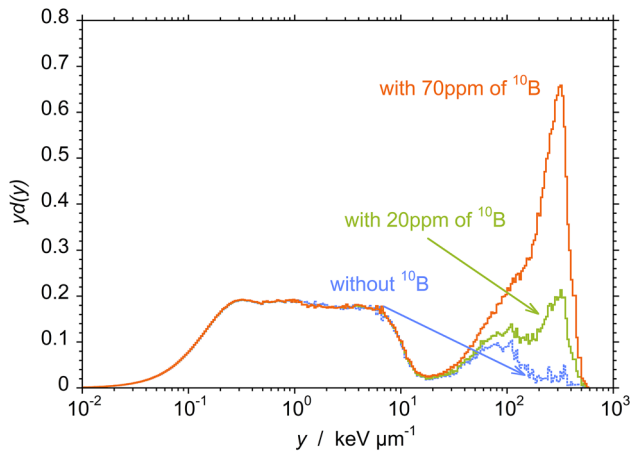


**Fig. 8** The microdosimetric distributions evaluated at 0, 20 and 70 ppm of  $^{10}\text{B}$

boronphenylalanine, which has demonstrated to ensure a safe and effective BNCT treatment [23, 24]. Maintaining a T/N ratio of at least 3.5:1 is considered a vital threshold to achieve the desired therapeutic outcomes.

Furthermore, achieving a sufficiently high concentration in the tumor is equally essential. Approximately  $10^9$  atoms of  $^{10}\text{B}$  per cell, equivalent to a concentration range of 20–50 ppm of  $^{10}\text{B}$ , are required to facilitate a substantial number of boron neutron capture reactions within a single cell. This high concentration is pivotal in guaranteeing the therapeutic effect and maximizing the potential for tumor cell destruction [24].

Figure 8 illustrates the impact of varying  $^{10}\text{B}$  concentrations (0, 20, and 70 ppm) on three distributions. The latter two distributions were derived from the 100 ppm distribution, accounting for individual components (photons, neutrons without boron, and BNC). The pure BNC component

**Table 1** The total and the individual dose components relative to the absorbed dose in case of no boron content, for boron concentrations of 0, 20 and 70 ppm

$^{10}\text{B}$ concentration/ ppm	$D_{tot}/D_0$	$D_{ph}/D_0$	$D_n/D_0$	$D_{BNC}/D_0$
0	1	0.85	0.15	0
20	1.17	0.85	0.15	0.17
70	1.59	0.85	0.15	0.59

was scaled based on the  $^{10}\text{B}$  concentration. Note that only the no-boron distribution  $d(y)$  is normalized to the unit dose, while the others are scaled to the no-boron spectrum for alignment with the gamma regions. The primary distinction is observed in the high lineal energy values (approximately 200 to 500  $\text{keV } \mu\text{m}^{-1}$ ), attributed to alpha particles and Li ions generated through the BNC reaction in the detector walls. These events overlap with contributions from residual fast neutrons and thermal neutron capture reactions in nitrogen, visible in the blue spectrum (without  $^{10}\text{B}$ ) above around 20  $\text{keV } \mu\text{m}^{-1}$ .

As illustrated in Fig. 6, the individual components contributing to the total dose can also be evaluated. This analysis is presented in Fig. 9 for 20 ppm of  $^{10}\text{B}$  (left) and 70 ppm of  $^{10}\text{B}$  (right). The total and individual dose components, relative to the absorbed dose in the absence of boron content,  $D_0$ , specifically the total dose  $D_{tot}/D_0$ , photon dose  $D_{ph}/D_0$ , neutron dose  $D_n/D_0$  and pure BNC dose  $D_{BNC}/D_0$ , are reported in Table 1.

The dose enhancement due to the addition of  $^{10}\text{B}$  amounts to 17% at 20 ppm and 59% at 70 ppm. To assess the biological impact, it is crucial to consider the increased biological effectiveness of high-LET particles. The distributions at 0, 20, and 70 ppm can be weighted using the Tilikidis weighting function to account for this. The resulting weighted distributions

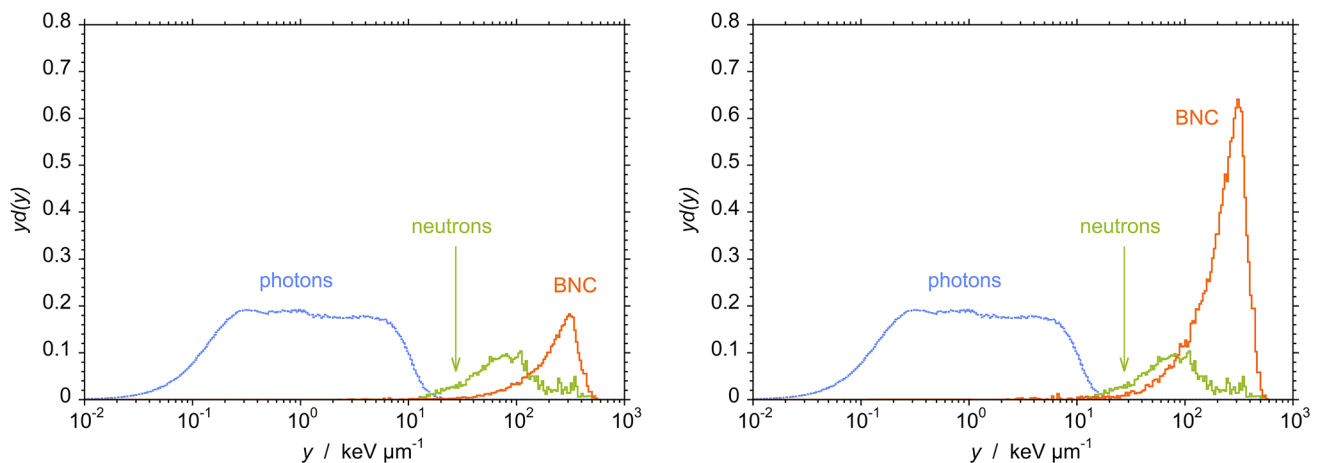


**Fig. 9** The individual photon, neutron and BNC components at 20 ppm (left) and 70 ppm (right) of  $^{10}\text{B}$

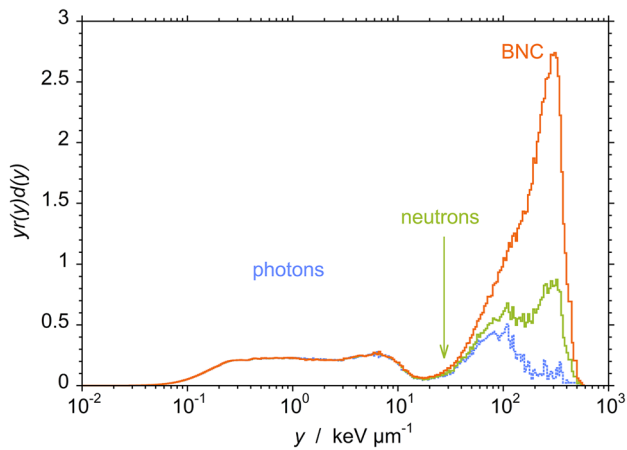


**Fig. 10** The microdosimetric distributions at 0, 20 and 70 ppm of  $^{10}\text{B}$ , weighted with the Tilikidis weighting function

are depicted in Fig. 10, where the integral under each curve corresponds to the RBE-weighted dose. The resulting values, relative to the physical dose without boron,  $D_0$ , are 1.7, 2.1 and 2.7 for 0, 20 and 70 ppm, respectively.

As a result of the weighting, the influence of the photon component decreases, while that of the alpha and lithium ions increases. If each individual distribution (photon, neutron, and BNC) is normalized to unity, Eq. (3) enables the calculation of the microdosimetric RBE for each component of the radiation field. The individual RBE values for the photon, neutron, and pure BNC components are 1.2, 4.2, and 4.4, respectively.

It is crucial to emphasize that the presented results are specific to the particular radiation field studied, and variations can be anticipated for different gamma/thermal and fast neutron/thermal neutron dose ratios. Furthermore, our investigation assumes a homogeneous distribution of  $^{10}\text{B}$  atoms within the walls of the sensitive volume, representing the cytoplasm surrounding critical nuclear structures. It is important to acknowledge that the actual scenario may differ significantly, considering the potential internal uptake of  $^{10}\text{B}$  atoms within the critical target. Notably, the measured BNC component with a TEPC uniquely corresponds to the cellular effect when  $^{10}\text{B}$  atoms are located in the tissue surrounding the sensitive target rather than within it. This uniqueness stems from the release of the BNC dose inside the cell, involving the simultaneous emission of two ions at an angle of  $180^\circ$ , presenting methodological challenges. The TEPC, designed to capture ionization events resulting from only one of the two ions produced in the A-150 walls, inherently yields event sizes generally smaller than those produced by BNC reactions within the biological target. Additionally, the potential existence of a heterogeneous distribution of the boron compound within cells and tissues introduces a complex dimension, leading to diverse biological outcomes [5].

## 4 Conclusion

Despite the acknowledged challenges related to the distribution of boron within and around biological targets, the microdosimetric approach stands as a powerful tool, offering critical insights into the intricate dynamics of Boron Neutron Capture Therapy (BNCT) within both cancerous and healthy tissues.

The potential applications of microdosimetry extend into the domain of treatment planning, providing opportunities for innovative strategies. Experimental microdosimetric spectra, measured at various depths within phantoms, serve as invaluable input data for advanced treatment planning methodologies [25].

To further explore the nuanced impact of different boron atom placements within biological tissue at the micrometer scale, especially considering heterogeneous distributions, we recommend the utilization of Monte Carlo simulations. These simulations offer a robust tool for comprehensive exploration and analysis. Additionally, the insights derived from Tissue-Equivalent Proportional Counter (TEPC) measurements play a crucial role in validating and refining Monte Carlo models, ensuring their accuracy and reliability in simulating the complex dynamics of BNCT.

Moreover, the inherent heterogeneity found in tumors, increasingly recognized as a major challenge in the treatment of solid tumors [26, 27], adds another layer of complexity. While replicating the real situation with experimental setups poses considerable challenges, microdosimetry, as a simplified model of reality, remains an essential tool for validating more versatile Monte Carlo models.

In conclusion, the application of microdosimetry in BNCT not only deepens our understanding of the underlying biological effects but also opens pathways for advancements in treatment planning and modeling. The integration of experimental data and sophisticated simulations is key to unlocking the full potential of BNCT as a targeted and effective cancer therapy.

**Authors' contributions** V. Conte: writing, conceptualization, review. A. Bianchi, A. Selva: data taking, revision of text.

**Funding** The research was supported by the fifth Commission of Istituto Nazionale di Fisica Nucleare (INFN).

**Availability of data and materials** On request.

**Code availability** Not applicable.

## Declarations

**Ethics approval** Not applicable.

**Consent to participate** Not applicable.

**Consent for publication** Not applicable.

**Conflict of interest** No conflict nor competing interests.

## References

- Goodhead DT. Initial events in the cellular effects of ionizing radiations: Clustered damage in DNA. *Int J Radiat Biol.* 1994;65(1):7–17. <https://doi.org/10.1080/09553009414550021>.
- ICRU Report 36. Microdosimetry. Bethesda, Maryland 20824: International Commission on Radiation Units and Measurements; 1983.
- Braby LA, Conte V, Dingfelder M, et al. ICRU report 98, stochastic nature of radiation interactions: Microdosimetry. *J ICRU.* 2023;23(1):1–168. <https://doi.org/10.1177/14736691231211380>.
- Nichols TL, Miller LF, Kabalka GW, Dudney TM. Microdosimetric study for interpretation of outcomes from boron neutron capture therapy clinical trials. *Radiat Prot Dosimetry.* 2007;126(1–4):645–7. <https://doi.org/10.1093/rpd/ncm130>.
- Sato T, Masunaga SI, Kumada H, Hamada N. Microdosimetric modeling of biological effectiveness for boron neutron capture therapy considering intra- and intercellular heterogeneity in  $^{10}\text{B}$  distribution. *Sci Rep.* 2018;8(1):988. <https://doi.org/10.1038/s41598-017-18871-0>.
- Hu N, Tanaka H, Takata T, Endo S, Masunaga S, Suzuki M, Sakurai Y. Evaluation of PHITS for microdosimetry in BNCT to support radiobiological research. *Appl Radiat Isot.* 2020;161:109148. <https://doi.org/10.1016/j.apradiso.2020.109148>.
- Wuu CS, Amols HI, Klianga P, Reinstein LE, Saraf S. Microdosimetry for boron neutron capture therapy. *Radiat Res.* 1992;130(3):355–9. <https://doi.org/10.2307/3578381>.
- Kota C, Maughan RL. A dosimetry system for boron neutron capture therapy based on the dual counter microdosimetric technique. *Bulletin du Cancer Radiotherapie.* 1996;83(Suppl):173s–5s. [https://doi.org/10.1016/0924-4212\(96\)84906-1](https://doi.org/10.1016/0924-4212(96)84906-1).
- Burmeister J, Kota C, Maughan RL, Waker AJ, Riley K, Wielopolski L. Application of TEPC microdosimetry to boron neutron capture therapy. *Radiat Prot Dosimetry.* 2002;99(1–4):351–2. <https://doi.org/10.1093/oxfordjournals.rpd.a006799>.
- Hsu FY, Hsiao HW, Tung CJ, Liu HM, Chou FI. Microdosimetry study of THOR BNCT beam using tissue equivalent proportional counter. *Appl Radiat Isot.* 2009;67(7–8 Suppl):S175–8. <https://doi.org/10.1016/j.apradiso.2009.03.043>.
- Endo S, Onizuka Y, Ishikawa M, Takada M, Sakurai Y, Kobayashi T, Tanaka K, Hoshi M, Shizuma K. Microdosimetry of neutron field for boron neutron capture therapy at Kyoto university reactor. *Radiat Prot Dosimetry.* 2004;110(1–4):641–4. <https://doi.org/10.1093/rpd/nch150>.
- De Nardo L, Seravalli E, Rosi G, Esposito J, Colautti P, Conte V, Torielli G. BNCT microdosimetry at the tapiro reactor thermal column. *Radiat Prot Dosimetry.* 2004;110(1–4):579–86. <https://doi.org/10.1093/rpd/nch206>.
- Moro D, Colautti P, Gualdrini G, Masi M, Conte V, De Nardo L, Torielli G. Two miniaturised TEPCS in a single detector for BNCT microdosimetry. *Radiat Prot Dosimetry.* 2006;122(1–4):396–400. <https://doi.org/10.1093/rpd/ncl484>.
- Moro D, Colautti P, Lollo M, Esposito J, Conte V, De Nardo L, Ferretti A, Ceballos C. BNCT dosimetry performed with a mini twin tissue-equivalent proportional counters (TEPC). *Appl Radiat Isot.* 2009;67(7–8 Suppl):S171–4.
- Colautti P, Moro D, Chiriotti S, Conte V, Evangelista L, Altieri S, Bortolussi S, Protti N, Postuma I. Microdosimetric measurements in the thermal neutron irradiation facility of LENA reactor. *Appl Radiat Isot.* 2014;88:147–52. <https://doi.org/10.1016/j.apradiso.2014.01.005>.
- Vohradsky J, Guatelli S, Davis JA, Tran LT, Rosenfeld AB. Evaluation of silicon based microdosimetry for boron neutron capture therapy quality assurance. *Physica Med.* 2019;66:8–14. <https://doi.org/10.1016/j.ejmp.2019.09.072>.
- Vohradsky J, Tran LT, Guatelli S, Chartier L, Vandevorde C, de Kock EA, Nieto-Camero J, Bolst D, Peracchi S, Höglund C, Rosenfeld AB. Response of SOI microdosimeter in fast neutron beams: Experiment and Monte Carlo simulations. *Physica Med.* 2021;90:176–87. <https://doi.org/10.1016/j.ejmp.2021.09.008>.
- Hu N, Tanaka H, Takata T, Okazaki K, Uchida R, Sakurai Y. Microdosimetric quantities of an accelerator-based neutron source used for boron neutron capture therapy measured using a gas-filled proportional counter. *J Radiat Res.* 2020;61(2):214–20. <https://doi.org/10.1016/j.apradiso.2009.03.042>.
- Selva A, Bellan L, Bianchi A, Giustiniani G, Colautti P, Fagotti E, Pisent A, Conte V. Microdosimetry of an accelerator based thermal neutron field for boron neutron capture therapy. *Appl Radiat Isot.* 2022;182:110144. <https://doi.org/10.1016/j.apradiso.2022.110144>.
- Selva A, Bianchi A, Bellan L, Fagotti E, Pisent A, Conte V. Comparison of biological weighting functions to estimate the microdosimetric RBE in BNCT. *Radiat Prot Dosimetry.* 2023;199(15–16):1963–7. <https://doi.org/10.1093/rpd/ncad007>.
- Conte V, Bianchi, A., Selva, A. Boron neutron capture therapy: Microdosimetry at different boron concentrations. *Appl Sci.* 2024;14(1):216. <https://doi.org/10.3390/app14010216>.
- Tilikidis A, Lind B, Nafstadus P, Brahme A. An estimation of the relative biological effectiveness of 50 MV bremsstrahlung beam by microdosimetric techniques. *Phys Med Biol.* 1996;41:55–69.
- Barth RF, Mi P, Yang W. Boron delivery agents for neutron capture therapy of cancer. *Cancer Commun (London, England).* 2018;38(1):35. <https://doi.org/10.1186/s40880-018-0299-7>.
- International Atomic Energy Agency. Advances in boron neutron capture therapy. IAEA, Vienna: Non-serial Publications; 2023.
- Sato T, Furusawa Y. Cell survival fraction estimation based on the probability densities of domain and cell nucleus specific energies using improved microdosimetric kinetic models. *Radiat Res.* 2012;178:341–56. <https://doi.org/10.1667/rr2842.1>.
- Marusyk A, Almendro V, Polyak K. Intra-tumour heterogeneity: A looking glass for cancer? *Nat Rev Cancer.* 2012;12(5):323–34.
- Bhatia S, Frangioni JV, Hoffman RM, Iafrate AJ, Polyak K. The challenges posed by cancer heterogeneity. *Nat Biotechnol.* 2012;30(7):604–10.

**Publisher's Note** Springer Nature remains neutral with regard to jurisdictional claims in published maps and institutional affiliations.

Springer Nature or its licensor (e.g. a society or other partner) holds exclusive rights to this article under a publishing agreement with the author(s) or other rightsholder(s); author self-archiving of the accepted manuscript version of this article is solely governed by the terms of such publishing agreement and applicable law.